

# Analysis of the mechanism of the accelerometer pre-buried method for a Depth of Penetration measurement

L. L. He, X. W. Chen & W. F. Xu  
*Institute of Systems Engineering,  
China Academy of Engineering Physics, China*

## Abstract

The pre-buried method has the potential to measure the Depth of Penetration (DOP) of a projectile into a target with a large dimension and potential dangers. Based on the numerical simulation of a reduced-scale projectile into unreinforced concrete target, the mechanism of the accelerometer pre-buried method is studied. The reasonable pre-buried location of the accelerometer is determined, the relationship between the target acceleration and the DOP of the projectile is constructed and the precision of the accelerometer pre-buried method is also discussed. Finally, the source of the maximum of target acceleration, i.e. the maximum radial expansion, is investigated.

*Keywords: mechanics of explosion, accelerometer pre-buried method, target acceleration, DOP of projectile, unreinforced concrete target.*

## 1 Introduction

Concrete is usually used in the civil and military structures, such as the underground command post, airplane garage, etc. All of these are vital targets to protect or attack. Since the Depth of Penetration (DOP) of projectile simultaneously represents the damage capabilities of the weapon and the anti-damage capabilities of the fortifications, it plays a key role in the designation of weapons and fortifications. In this way, the technology for DOP measurement becomes a significant problem. It is noted that the unreinforced concrete target is specified in the present manuscript except special explanations.

Up to now, the methodology of DOP measurement includes direct method and indirect method.



The direct method measures the length of penetration channel with rulers, which is convenient and robust. However, limited by the length of the ruler in reality, it is difficult to measure the deep penetration channel in large target. On the other hand, it requires staff to carry on the measuring near the penetration site, which has huge potential dangers if the explosive loaded in projectile hangs fire. Meanwhile, the channel must be cleared up; the target should even be sectioned, which is time-consuming and high-cost. Therefore, the direct method is usually used in the lab tests for reduced-scale projectile and no explosives are loaded.

The indirect method firstly measures other parameters, and then obtains the DOP of projectile according to its relationship with the measured parameters. Therefore, the relationship has significant importance in the indirect method. Commonly, the indirect method includes the acceleration-integral method, detection method, pre-buried method, and so on.

The acceleration-integral method obtains the DOP of projectile by integrating the time history of projectile acceleration during penetration. The projectile acceleration could be obtained by the accelerometer loaded in the projectile. However, the corresponding technology is pre-mature up to now (He *et al.* [1]). It may be difficult to obtain the projectile acceleration, especially when the target is multi-layered, or the scale of projectile is small. For the defence side, this method could not be used to estimate the damage of fortifications. Therefore, the acceleration-integral method is usually used in the depth-control fuse in order to locate its triggering location (Ma *et al.* [2]).

The detection method is non-destructive, which obtains the DOP of projectile based on the characteristics of the propagation of sonic, optical, electric or magnetic signal, such as the Ground Penetrating Radar (GPR), supersonic or X-ray equipments. However, the attenuation and diffusion may disturb the propagation of signals, especially when the target is large and complex. The worker should measure on site, either. Similar to the direct method, the detection method is often used in the reduced-scale lab tests.

The pre-buried method arranges a series of sensors in the target prior to penetration, and the sensor is triggered when the projectile achieves a certain depth, such as the studies, [3–5]. The DOP of projectile could be obtained according to the response and arrangement of sensors. Eichelberger [6] and Allen *et al.* [7] respectively obtained the DOP of projectile into metallic and soil targets. Compared to the aforementioned methods, the pre-buried method is independent of the dimension of target and projectile, and the staff need not work on site. These merits make it the reasonable method for DOP measuring in large and dangerous targets.

However, the traditional pre-buried method requires the sensors must be arranged in the penetration channel. This needs precise prediction of the ballistic trajectory of projectile before tests, which is usually unavailable. It is necessary to develop a new pre-buried method, which could have the sensors arranged away from the penetration channel. The accelerometer pre-buried method is the very one. It measures the local acceleration of target and derives the DOP of projectile according to the target response. Therefore, the key is to find the

reasonable pre-buried location of accelerometers and construct the relationship between the acceleration of local target and DOP of projectile.

Compared to the experimental method (He [8]), numerical simulation could easily obtain the instantaneous parameters during penetration, including the distribution of stress and acceleration of target and projectile, etc. Hence, the numerical method is employed in the present manuscript.

Since the pre-buried method is independent of the dimension of target and projectile, only reduced-scale projectile and target is studied in the present manuscript for saving computational expense.

Based on ANSYS/LS-DYNA, the penetration process of projectile into unreinforced concrete target is simulated. According to the simulation results, the principle and location of pre-buried accelerometer is discussed, the relationship between the local acceleration of target and DOP of projectile is constructed, and the precision of the accelerometer pre-buried method is studied.

## 2 Numerical simulation of penetration process

The projectile normally penetrates into the cylindrical unreinforced concrete target. The scheme of target and projectile is shown in fig. 1. The origin of the fixed coordinates is the striking point of projectile and target. The X axis goes outward of the perpendicular direction of the paper plane. The penetration direction is along the positive Y axis.

The dimension of projectile and target is listed in table 1. Since the ratio between the diameters of concrete and projectile is 25.6, the target could be approximated as semi-infinite. Specifically, the dimension of target is required to be large enough to approximate it as semi-infinite, in case the concrete target crushes during penetration.

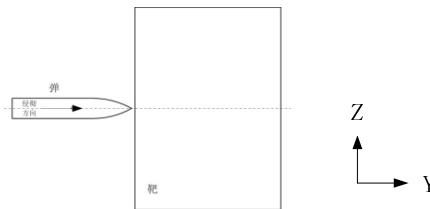


Figure 1: Scheme of projectile and target.

Table 1: Dimension of projectile and target.

Long-rod hollow projectile with ogival nose				
Diameter $d_p$ (mm)	Length $L_p$ (mm)	$L_p / d_p$	CRH	Mass (kg)
25	200	8	3	0.41
Cylindrical unreinforced concrete target				
Length $L_t$ (mm)		Diameter $d_t$ (mm)		Penetration direction
768		640		Y+

The projectile material is high-strength alloy steel. The projectile is assumed as rigid, for the mechanical deformation of projectile is pretty small. The material parameters are listed in table 2. The hollow projectile is equivalent to solid one according to the same mass.

The Holmquist Johnson Concrete (HJC) model [9] is adopted to represent the mechanical behaviour of unreinforced concrete. Table 3 lists the corresponding parameters, which are determined based on the study [10].

Since the geometries and loads of target and projectile are symmetrical, the half model is constructed, and the symmetrical boundary conditions are applied. Element SOLID 164 is adopted to mesh the projectile and target. The mesh size is refined along the penetration path, and the diameter of the refined part is almost 3 times of projectile diameter, for the penetration tests demonstrate that the damage is localized in this area (He *et al.* [11]). The Surface-to-surface contact algorithm is employed. The scale coefficient of time step size is 0.7.

Table 2: Material parameters for projectile material.

Rigid model		
Equivalent density $\rho_t$ (kg/m <sup>3</sup> )	Young's modulus $E$ (GPa)	Poisson's ratio
4668	210	0.3

Table 3: Parameters for HJC model.

	Density (kg/m <sup>3</sup> )	2400
	Shear modulus (GPa)	11.94
Strength parameters	$A$	0.79
	$B$	1.6
	$N$	0.61
	$C$	0.007
	Unconfined compressive strength (MPa)	30
	$S_{max}$	7.0
	$T$ (MPa)	3.34
Damage parameters	$D_1$	0.04
	$D_2$	1.0
	$EF_{min}$	0.01
Pressure parameters	$P_{crush}$ (MPa)	10
	$\mu_{crush}$	0.00074
	$K_1$ (GPa)	85
	$K_2$ (GPa)	-171
	$K_3$ (GPa)	208
	$P_{lock}$ (MPa)	800
	$\mu_{lock}$	0.12



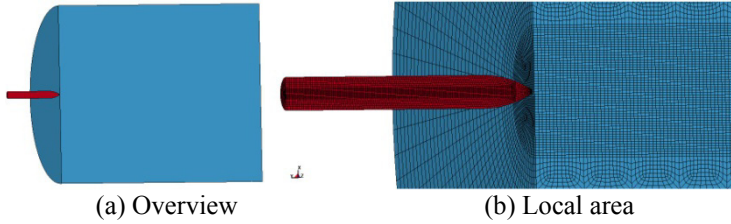


Figure 2: Meshes of the projectile and target.

Figure 3 shows the time history of DOP respectively obtained by numerical simulation (dash black line) and rigid-penetration model prediction [12–14] (solid red line) at striking velocity 720 m/s. The time is represented by the instant penetration velocity. It is obvious that the two coincide well with each other. The numerical analysis could also obtain the instantaneous penetration velocity and acceleration of projectile and the local acceleration of target, etc.

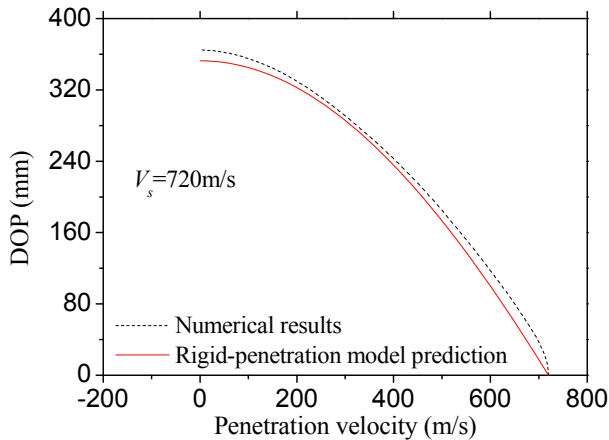
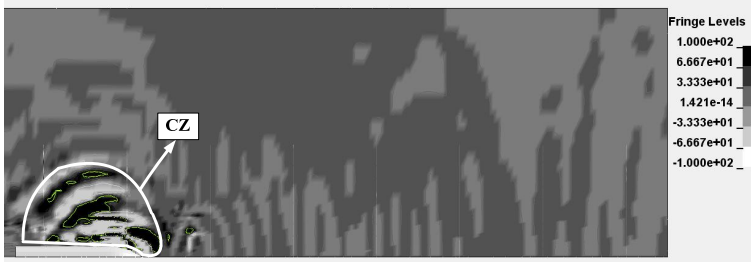


Figure 3: Comparison of time history of DOP of projectile between the numerical analysis and rigid-penetration model prediction [12–14].

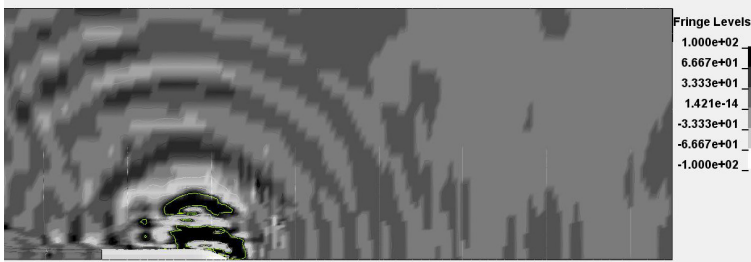
### 3 Pre-buried location of the accelerometer

Figure 4 shows the radial acceleration of local target obtained by the numerical simulation in the plane  $X = 0$  mm at different time. Except special notation, the target acceleration indicates the radial acceleration of local target. It is illustrated that the absolute value of target acceleration is much larger around the projectile nose than in other place of target. The specific area is denoted as the Characteristic Zone (CZ), as shown in fig. 4a. Obviously, the CZ is always around the projectile nose tip with the penetration progressing. Beyond the CZ, the target acceleration dramatically decreases, and its distribution tends to be chaos near the boundary of target.

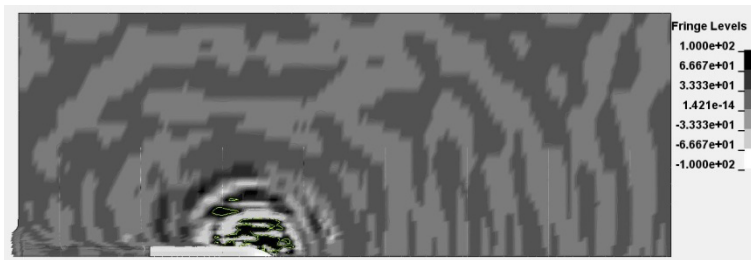
Figure 5 shows the maxima of target acceleration for several points along the line  $X = 0$  mm and  $Y = 250$  mm. Here  $|Z|$  is the radial distance from the point to the penetration path. As shown in fig. 5, the exponential decaying is obvious for the maximum of target acceleration.



(a)  $t = 0.3$  ms



(b)  $t = 0.6$  ms



(c)  $t = 0.9$  ms

Figure 4: Distribution of target acceleration in the plane  $X = 0$  mm at different time. The unit of the fringe level is 100 g.

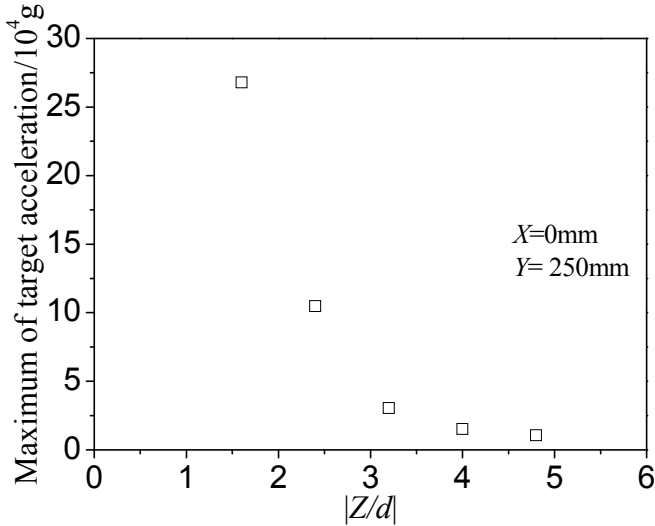


Figure 5: Maxima of target acceleration with the radial distance from the penetration channel changing.

Based on the experimental analysis, the concrete target is divided into three zones from the penetration channel to the boundary layer, i.e. the comminution zone, the fracture zone and the elastic deformation zone. The damage of target could be represented by the damage parameter  $D$ .  $D = 1$  indicates that the target is totally damaged, corresponding to the comminution zone,  $0 < D < 1$  indicates that there is damage in target, corresponding to the fracture zone, and  $D = 0$  indicates the target has no damage, corresponding to the elastic deformation zone. The distribution of the damage parameter is shown in fig. 6 for the target. The diameter of the damage zone is approximately 160 mm, which is about 3 times of the projectile diameter.

In reality, the accelerometer is pre-buried in the concrete target in order to measure the target acceleration. According to the analysis above, since the perturbation of target acceleration is chaos far away from the penetration, the accelerometer should be pre-buried as near as enough to the penetration channel. However, the accelerometer may untie from the target in the comminution zone or the fracture zone, which could induce wrong testing results for the target acceleration. Therefore, the best option is to pre-bury the accelerometer in the boundary of the elastic deformation zone and the fracture zone, which is about 3 to 4 times of the projectile diameter away from the penetration channel. In the present manuscript, the line  $X = 0$  mm and  $Z = 100$  mm is chosen to be the location where the accelerometer is pre-buried.

The even space between the accelerometer along the penetration path controls the precision of the measurement, which will be further discussed in the following section. The space is 50 mm in the present manuscript.

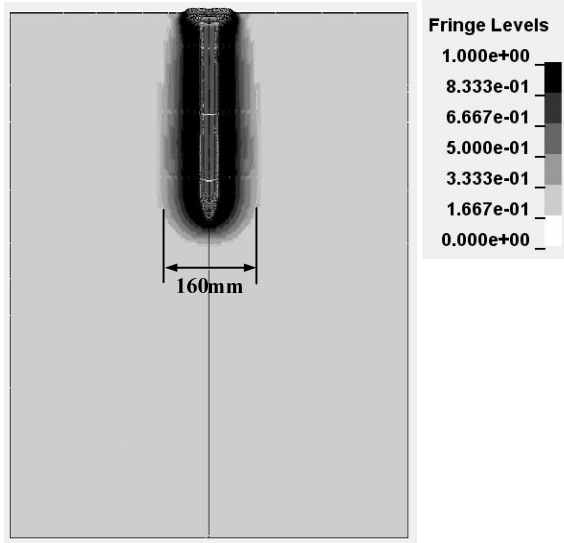


Figure 6: Distribution of target damage at certain time.

#### 4 Relationship between target acceleration and DOP of projectile

Figure 7 shows the time history of target acceleration at point  $(X, Y, Z) = (0 \text{ mm}, 250 \text{ mm}, 100 \text{ mm})$ . Three time points are labelled in the figure, i.e. Time I: the time the DOP of nose tip reaches 250 mm; Time II: the time the DOP of transition from shank to nose achieves 250 mm; Time III: the time the maximum of target acceleration appears. Through comparison of these three time points, Time III approximately coincides with Time II, but it has a large deviation from Time I. Therefore, the DOP of transition from nose to shank is 250 mm as soon as Time III reaches. The instant DOP of projectile is  $250 \text{ mm} + 41 \text{ mm} = 291 \text{ mm}$ . Here 41 mm is the length of projectile nose. Within the ultimate DOP of projectile, the above analysis constructs a relationship between the instant DOP of projectile and the target acceleration.

Beyond the ultimate DOP of projectile, the maximum of target acceleration should dramatically decrease according to fig. 4.

The maxima of target acceleration along the line  $X = 0 \text{ mm}$  and  $Z = 100 \text{ mm}$  are shown in fig. 8. It firstly has an increasing trend and then dramatically decreases along the line. Quantitatively, we define a decrease larger than 50% as a dramatic decrease, noted as 50% reduction.  $Y = 300 \text{ mm}$  is the location where the 50% reduction occurs in fig. 8. The target is divided into effective penetration zone and non-penetration zone by the plane  $Y = 300 \text{ mm}$ , as shown in fig. 8. According to the analysis above, the ultimate DOP of projectile is  $300 \text{ mm} + 41 \text{ mm} = 341 \text{ mm}$ , which is just -6.58% deviated from the result of numerical simulation 365 mm, as shown in fig. 2.

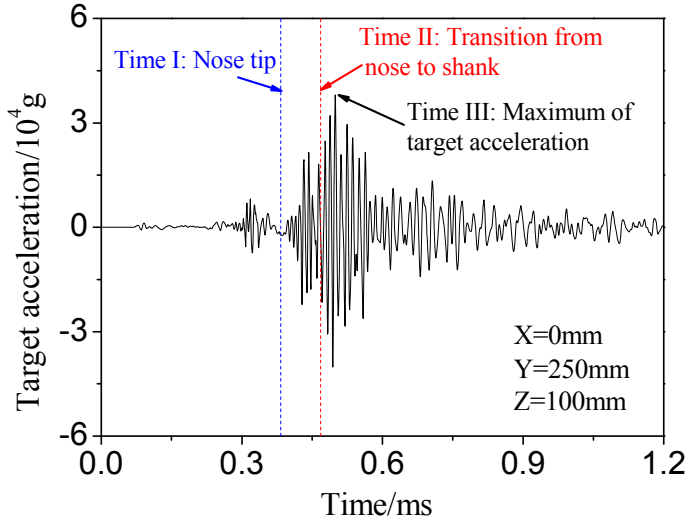


Figure 7: Time history of target acceleration at point  $(X, Y, Z) = (0 \text{ mm}, 250 \text{ mm}, 100 \text{ mm})$ .

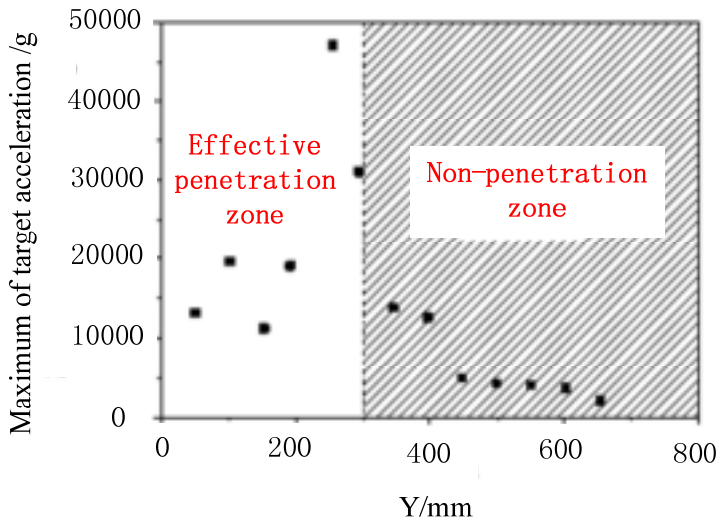


Figure 8: Maxima of target acceleration along the line  $X = 0 \text{ mm}$  and  $Z = 100 \text{ mm}$ .

It should be noted that the space of accelerometer along the penetration path determines the precision of the accelerometer pre-buried method. The space is 50 mm in the present manuscript, and the precision is  $\pm 13.7\%$ . Hence, if the

precision  $\alpha\%$  is required, the space should be less than  $100Z_r / \alpha$ , in which  $Z_r$  is the ultimate DOP of projectile. In the engineering applications, the ultimate DOP of projectile could be estimated by the empirical formula.

In this way, the mechanism of accelerometer pre-buried method is analyzed. As long as the accelerometer is pre-buried in reasonable location, the time history of target acceleration could be recorded, and the DOP of projectile could be derived according to the mechanism above.

## 5 Discussions

According to the above analysis, Time II and Time III coincide well in fig. 7 and this coincidence is extrapolated to any time and any pre-buried location during penetration. Hence, the maximum expansion should be specifically located in order to explain the reason.

Approximately, we could think the maximum of target acceleration corresponds to the maximum force in  $Z$  direction exerted by the projectile. Assuming the projectile as rigid, the force on each point of projectile outer surface could be expressed as follows in  $Z$  direction according to the dynamic cavity-expansion theory [13, 14].

$$f_z = (R + \rho_t v^2 \sin^2 \theta) \cos \theta \quad (1)$$

where  $R$  is the dynamic compressive strength of concrete,  $v$  is the instant penetration velocity of projectile, and  $\theta$  is the angle between the tangential line of projectile outer surface and the axis of projectile.  $0^\circ \leq \theta \leq 56.5^\circ$  for the projectile in the present manuscript.

If both  $\partial f_z / \partial \theta = 0$  and  $\partial^2 f_z / \partial \theta^2 < 0$  are satisfied,  $f_z$  gets its maximum value. According to eqn. (1), we have

$$\frac{\partial f_z}{\partial \theta} = -\frac{R}{3\rho_t v^2} - \frac{1}{3} + \cos^2 \theta \quad (2)$$

$$\frac{\partial^2 f_z}{\partial \theta^2} = -2 \sin \theta \quad (3)$$

Apparently, eqn. (3) always stands for the projectile in the present manuscript. If  $0 < R \leq 2\rho_t v^2$ , i.e.  $v \geq \sqrt{R/2\rho_t}$ ,  $\partial f_z / \partial \theta = 0$  could be obtained and the maximum expansion exerted by the point with  $\theta = \cos^{-1} \sqrt{R/3\rho_t v^2 + 1/3}$ . If  $R > 2\rho_t v^2$ , i.e.  $v < \sqrt{R/2\rho_t}$ ,  $\partial f_z / \partial \theta < 0$  always stands, and the maximum expansion exerted by the transition from nose to shank.

For the projectile in the present manuscript, if  $v \leq \sqrt{R/2\rho_t} = 286\text{m/s}$ , the maximum expansion is exerted by the transition from nose to shank; if

$v \geq 499\text{m/s}$ , it is exerted by the nose tip of projectile; if  $286\text{m/s} < v < 499\text{m/s}$ , it is exerted by the point between the nose tip and transition from nose to shank.

However, time is needed to translate the expansion from the penetration channel to the point the target acceleration is recorded. This indicates that the maximum of target acceleration could only be reached after the maximum expansion is exerted by the projectile nose.

Based on the aforementioned analysis, the deviation between Time I and Time III should increase with penetration progressing, and the deviation between Time II and Time III, which would firstly decrease and then increase, is much smaller than that of Time I and Time III. Therefore, it is reasonable to assume Time II and Time III coincide well during the whole penetration process.

## 6 Conclusions

Based on the numerical simulation, the mechanism of accelerometer pre-buried method is studied. The best option is to pre-bury the accelerometer in the boundary of the elastic zone and the fracture zone of concrete target, which is 3 to 4 times of the projectile diameter away from the penetration channel. Within the DOP of projectile, the time the maximum of target acceleration appears approximately coincides with the time the transition from nose to shank penetrates into the pre-buried depth of the accelerometer. Beyond the DOP of projectile, the maximum of target acceleration significantly decreases. With the depth of the pre-buried accelerometer increasing, the maxima of target acceleration firstly increase and then dramatically decrease. The 50% reduction is defined to divide the target into effective penetration zone and the non-penetration zone. The ultimate DOP of projectile is the sum of the depth of the boundary of the two zones and the length of projectile nose. The precision of the accelerometer pre-buried method is controlled by the space of the accelerometer along the penetration path. Furthermore, the maximum expansion, which induces the maximum of target acceleration, is discussed. It gradually translates from the transition from nose to shank to the nose tip with the penetration velocity increasing. In a word, the analysis could provide basis for the engineering application of the accelerometer pre-buried method in the future, especially when the target is large and dangerous.

## Acknowledgements

This work is supported by the National Outstanding Young Scientists Foundation of China (Grant No. 11225213) and Programs of National Natural Science Foundation of China (Grant Nos. 11172282, 11302210 and 11390362).

## References

- [1] He, L.L., Gao, J.Z. & Chen, X.W. Experimental study on measure technology of projectile deceleration. *Explosion and Shock Waves*, **33(6)**, pp. 2013 (in Chinese).



- [2] Ma, B.C., Cao, H.S., Zhang, Y., Lu, L.J. & Zhang, J.F. The numerical study on penetration depth confirmation based on overload information. *Journal of Projectiles, Missiles and Guidance*, **31(6)**, pp. 79-82, 2011 (in Chinese).
- [3] Lawrence, W. Measurements of Penetration using Instrumented Targets, in *Shock Waves in Condensed Matter*, 1987 [M]. Elsevier Science Publisher B. V., pp. 745-748, 1988.
- [4] Peters, J., Anderson, W.F. & Watson A.J. Development of Instrumentation Techniques to Investigate High Velocity Projectile Penetration into Construction Materials. *Proceedings of the Sixth International Symposium on Interaction of Nonnuclear Munitions with Structures*. Panama City Beach, Florida, pp. 23-28, 1993.
- [5] Gold, V.M., Vradis, G.C. & Pearson, J.C. Concrete penetration by eroding projectiles: Experiments and analysis. *Journal of Engineering Mechanics-ASCE*, **122(2)**, pp. 145-152, 1996.
- [6] Eichelberger, R.I. Experimental test of the theory of penetration by metallic jets. *Journal of Applied Physics*, **27**, pp. 63-68, 1956.
- [7] Allen, W.A., Mayfield, E.B. & Morrison, H.L. Dynamics of a projectile penetrating sand. *Journal of Applied Physics*, **28**, pp. 370-376, 1957.
- [8] He, L.L. *Studies on Dynamic Behavior of High-speed Projectile Penetrating into Concrete Target – Considering Mass Loss and Nose Blunting*. Ph. D. Thesis, University of Science and Technology of China, 2012 (in Chinese).
- [9] Holmquist, T.J. & Johnson, G.R. A computational constitutive model for concrete subjected to large strains, high strain rates, and high pressures. Presented at *14th International Symposium on Ballistics*, Quebec City, Canada, September 1993.
- [10] Zhang, F.G. & Li, E.Z. A method to determine the parameters of the model for concrete impact and damage. *Proceedings of the symposium on penetration of materials*, pp. 188-193, 2001 (in Chinese).
- [11] He, X., Xu, X.Y., Sun, G.J., Shen, J., Yang, J.C. & Jin, D.L. Experimental investigation on projectiles' high-velocity penetration into concrete targets. *Explosives and Shock Waves*, **30(1)**, pp. 1-6, 2010 (in Chinese).
- [12] Forrestal, M.J. & Altman, B.S. *An Empirical Equation for Penetration Depth of Ogive Nose Projectile into Concrete Targets*. SNL: USA, SAND29221948C, 1993.
- [13] Chen, X.W. & Li, Q.M. Deep penetration of a non-deformable projectile with different geometrical characteristics. *International Journal of Impact Engineering*, **27(6)**, pp. 619-637, 2002.
- [14] Li, Q.M. & Chen, X.W. Dimensionless formulae for penetration depth of concrete target impacted by a non-deformable projectile. *International Journal of Impact Engineering*, **28(1)**, pp. 93-116, 2003.